

Histone Variant H2A.Z Marks the 5' Ends of Both Active and Inactive Genes in Euchromatin

Ryan M. Raisner,^{1,4} Paul D. Hartley,^{1,4}
Marc D. Meneghini,¹ Marie Z. Bao,¹ Chih Long Liu,²
Stuart L. Schreiber,² Oliver J. Rando,²
and Hiten D. Madhani^{1,*}

¹Department of Biochemistry and Biophysics
University of California
600 16th Street

San Francisco, California 94143

²Bauer Center for Genomics Research
Harvard University

7 Divinity Avenue

Cambridge, Massachusetts 02138

Summary

In *S. cerevisiae*, histone variant H2A.Z is deposited in euchromatin at the flanks of silent heterochromatin to prevent its ectopic spread. We show that H2A.Z nucleosomes are found at promoter regions of nearly all genes in euchromatin. They generally occur as two positioned nucleosomes that flank a nucleosome-free region (NFR) that contains the transcription start site. Astonishingly, enrichment at 5' ends is observed not only at actively transcribed genes but also at inactive loci. Mutagenesis of a typical promoter revealed a 22 bp segment of DNA sufficient to program formation of a NFR flanked by two H2A.Z nucleosomes. This segment contains a binding site of the Myb-related protein Reb1 and an adjacent dT:dA tract. Efficient deposition of H2A.Z is further promoted by a specific pattern of histone H3 and H4 tail acetylation and the bromodomain protein Bdf1, a component of the Swr1 remodeling complex that deposits H2A.Z.

Introduction

The association of eukaryotic DNA with histone octamers to form nucleosomes has profound implications for all aspects of DNA metabolism. Epigenetic control mediated through chromatin is now recognized as a major form of genetic regulation that functions during both normal development and pathogenic processes such as tumorigenesis. Therefore, a critical challenge faced by dividing eukaryotic cells is the faithful maintenance of both active and inactive epigenetic states of specific genomic regions. Three known biochemical mechanisms exist to control the states of chromatin: histone posttranslational modifications (on both the unstructured N-terminal tails and core regions), ATP-dependent chromatin remodeling by Swi2/Snf2 family members, and histone variant substitution. The current goal of the field is to link these mechanisms to epigenetic regulation. Substantial progress has been made in understanding how silent heterochromatin is generated and maintained. Compared to heterochromatin, less is

understood about how euchromatin is generated, maintained, and inherited. Indeed, euchromatin has widely been viewed as a default state. More recently, however, several chromatin modifications have been identified that promote the euchromatic state by antagonizing silencing. These include the replacement of histone H2A by H2A.Z (Meneghini et al., 2003) and three histone modifications: acetylation on lysine 16 of the H4 tail (Kimura et al., 2002; Suka et al., 2002) and methylation of lysines 4 and 79 of H3 (Ng et al., 2003a; Santos-Rosa et al., 2004; van Leeuwen et al., 2002). In this paper, we focus on the deposition pattern of H2A.Z in euchromatin and its implications.

In previous work, we demonstrated that in *S. cerevisiae*, the evolutionarily conserved histone variant H2A.Z functions in euchromatin to antagonize the spread of Sir-dependent silencing. Furthermore, we showed that at the right border of the *HMRa* silent mating-type cassette, H2A.Z functions in parallel with a well-characterized boundary element (Meneghini et al., 2003). Thus, H2A.Z is a component of euchromatin that functions to antagonize the opposite chromatin state. One key question, therefore, is whether H2A.Z is randomly distributed through euchromatin and if not, how its deposition to specific sites is determined. We and others have also identified a 13 subunit ATP-dependent chromatin remodeling complex, the Swr1 complex, that is required for the deposition of H2A.Z in vivo (Kobor et al., 2004; Krogan et al., 2003b; Mizuguchi et al., 2004). Where the Swr1 complex acts and how its specificity is determined is not known. A subunit of this complex is Bdf1, a protein containing two tandem bromodomains known to bind acetylated histone tails (Ladurner et al., 2003; Matangkasombut and Buratowski, 2003). This suggests recognition of histone acetylation as one potential mechanism for the targeting of H2A.Z deposition to euchromatin.

Early chromatin immunoprecipitation (ChIP) experiments performed by Smith and coworkers suggested a relative enrichment of an epitope-tagged version of H2A.Z at the promoter regions of the highly inducible *GAL1–10* and *PHO5* genes in yeast (Santisteban et al., 2000). Moreover, these experiments demonstrated enrichment under noninducing conditions for the linked genes, and this enrichment decreased upon gene induction. However, it is difficult to make general conclusions from these studies for three reasons. First, since only four intergenic regions were examined, their correlation with higher H2A.Z levels could have been coincidental. Second, since no intergenic regions lacking a promoter were examined, the correlation with H2A.Z levels could have reflected preferential H2A.Z deposition in intergenic regions rather than in promoters per se. Third, since nucleosome density was not examined in the gene induction experiments, whether H2A.Z was selectively removed upon gene activation relative to H3, for example, was not clear. Thus, the following issues remain unresolved: (1) where is H2A.Z deposited in general?, (2) what is the relationship between H2A.Z

*Correspondence: hiten@biochem.ucsf.edu

⁴These authors contributed equally to this work.

deposition to transcription?, and (3) what are the signals that induce its deposition?

Results

H2A.Z Is Preferentially Enriched at 5' Regions in General

Previous studies have described a prominent role for H2A.Z at heterochromatin-proximal regions to antagonize the spread of silencing; however, we were curious to examine whether H2A.Z might play a broader role in the genome. Such additional roles could be elucidated through knowledge of the deposition profile of H2A.Z across chromosomes. We chose to examine the H2A.Z deposition profile in *S. cerevisiae* chromosome III because it contains the *HMRa* and *HMLα* silent mating-type cassettes and is well characterized with respect to the location of replication origins, cohesion sites, and transcription initiation sites. This analysis was conducted with a strain carrying an allele of H2A.Z with an amino-terminal influenza hemagglutinin epitope tag (*HA₃-HTZ1*) that was integrated at the endogenous locus as the sole genomic copy. This allele is functional in that it can complement the synthetic lethality of *htz1Δ* with *bre1Δ* (Hwang et al., 2003). ChIP and quantitative real-time PCR (QPCR) were used to determine H2A.Z enrichment at 300 bp segments whose 5' ends were spaced at 1000 bp intervals across chromosome III. We observed a highly nonuniform and chromosome-wide distribution of H2A.Z (Figure 1A; see Table S1 in the Supplemental Data available with this article online). Further analysis of our data indicated that the level of H2A.Z deposition at a given ChIP probe region was positively correlated with its proximity to the nearest 5' end of a gene (Figure 1B). However, we observed no apparent correlation with proximity to 3' ends of genes that are not near 5' ends, the transcription rate of the nearest gene, cohesion sites, or origins of replication (M.Z.B., M.D.M., and H.D.M., unpublished data and see below).

We next increased the resolution of our chromosome III analysis to a single intergenic region flanked by two nonconverging ORFs. The intergenic region upstream of *SNT1* was chosen because it is significantly smaller relative to the *SNT1* coding region. A 4.2 kb continuous region starting from 2 kb upstream of the *SNT1* initiation codon to 2.2 kb downstream was assayed for H2A.Z enrichment by ChIP and QPCR using primer sets that tiled the region. This assay revealed a striking intergenic enrichment for H2A.Z with a sharp decline in the coding region of *SNT1* and in the upstream gene *BPH1* (Figure 1C).

We then identified a larger region of chromosome III (the *LEU2-YCL012W* interval) containing a mixture of gene orientations: genes whose 5' ends share an intergenic region (5'-5'); genes whose 5' ends are adjacent to a 3' end (5' only); and genes whose 3' ends converge (3'-3'). We assayed the H2A.Z deposition profile within this 11 kb region by ChIP and QPCR. This tiling analysis revealed that for every H2A.Z peak of enrichment, there was a corresponding 5' end (Figure 1D). In most cases, the peak enrichment of H2A.Z was close to or directly upstream of the initiation codon. The only

shared 5' region in this data set (the *DCC1-BUD3* intergenic region) had two distinct peaks of H2A.Z enrichment, one corresponding to the 5' end of each gene. The observed H2A.Z peaks in these promoter regions were not due to increased crosslinkability or nucleosome density of these regions because additional ChIP analysis of histone H3 across the same region revealed slightly lower, not higher, ChIP signals in intergenic regions (Figure S1). Finally, the two regions with converging ORFs (3'-3') had no observable peak of H2A.Z, supporting the notion that H2A.Z is indeed selectively enriched at 5' regions of genes.

High-Resolution Chromosome-Wide Mapping of Endogenous H2A.Z Nucleosomes

Our initial analyses of H2A.Z deposition relied on a ChIP protocol that involved shearing DNA to an average size of 500 bp, which meant that QPCR analyses of immunoprecipitated material resolved multiple nucleosomes, thereby obscuring finer details of H2A.Z localization. In addition, the tiling methods we used to assay H2A.Z deposition at an appropriate resolution are not feasible for rapidly examining much larger regions such as whole chromosomes. To overcome these two limitations, we used a ChIP and microarray hybridization protocol to analyze the distribution of endogenous, untagged H2A.Z at the resolution of single nucleosomes; the data were normalized for nucleosome density (see Experimental Procedures). The microarrays tiled the majority of chromosome III and 223 additional regulatory regions at a resolution of 20 bp. These experiments yielded a nucleosome-resolution map of H2A.Z enrichment patterns across nearly half a megabase of the *S. cerevisiae* genome (Table S2).

Analysis of the data recapitulated our initial conclusions about the specific deposition of H2A.Z at 5' ends of genes (Figure 1) and extended these conclusions to a larger portion of the yeast genome. Figure 2A shows the microarray data for the regions analyzed by QPCR in Figures 1C and 1D. Consistent with the QPCR data, the region upstream of *SNT1* contains H2A.Z, and this H2A.Z signal has now been resolved into a striking distribution pattern in which two consecutive nucleosomes contain H2A.Z. Two H2A.Z nucleosomes are also found upstream of the *BPH1* gene, one upstream of the *FEN1* gene and two in the *RRP43-RBK1* intergenic region that is flanked by the 5' ends of the respective genes. In contrast, no H2A.Z peak was observed in the *FEN1-RRP43* intergenic region that is flanked by the 3' ends of those two genes. Also shown in Figure 2A is a portion of the *NFS1-YCL012C* region analyzed in Figure 1D; *LEU2* is missing because this gene is deleted in the strain profiled using the microarray method. The QPCR analysis of this region was precisely recapitulated by the microarray data: H2A.Z was found specifically in intergenic regions that contain at least one 5' end of a gene. Indeed, analysis of the entirety of chromosome III revealed H2A.Z upstream of most euchromatic genes and not at intergenic regions flanked by two converging 3' ends (Table S2). Genes on chromosome III that lacked detectable H2A.Z in their promoter regions correspond to genes in the *HMLα* silent cassette, genes near the telomeres of chromosome

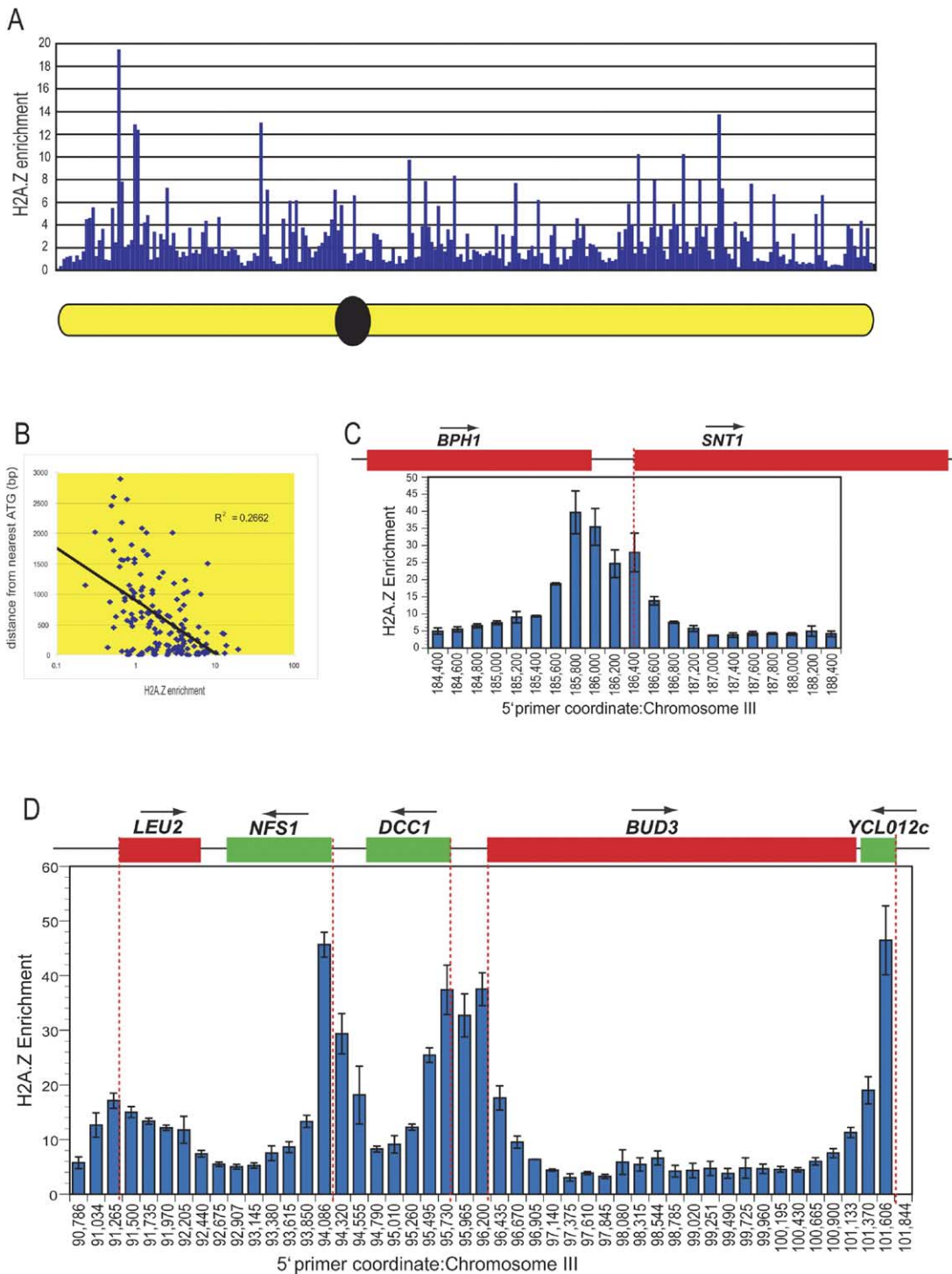


Figure 1. H2A.Z Enrichment in Euchromatin

(A) Schematic of HA₃-Htz1 ChIP enrichment across chromosome III. Bars represent IP/WCE value as determined by QPCR for a single 300 bp segment. Each 5' primer is separated by 1000 bp.

(B) Log scale graph comparing H2A.Z enrichment values to distance to the nearest initiation codon. The correlation coefficient is 0.2662.

(C and D) Diagram of *BPH1-SNT1* interval (C) and the *LEU2-YCL012c* interval (D). Both regions were assayed by ChIP and QPCR for HA₃-Htz1 deposition. Enrichment values are average IP/WCE ratios from triplicate samples with standard error of the mean (SEM) error bars. Vertical dashed lines are drawn through each gene's initiation codon. x axis values are the chromosomal coordinates of the 5' primers of each pair used.

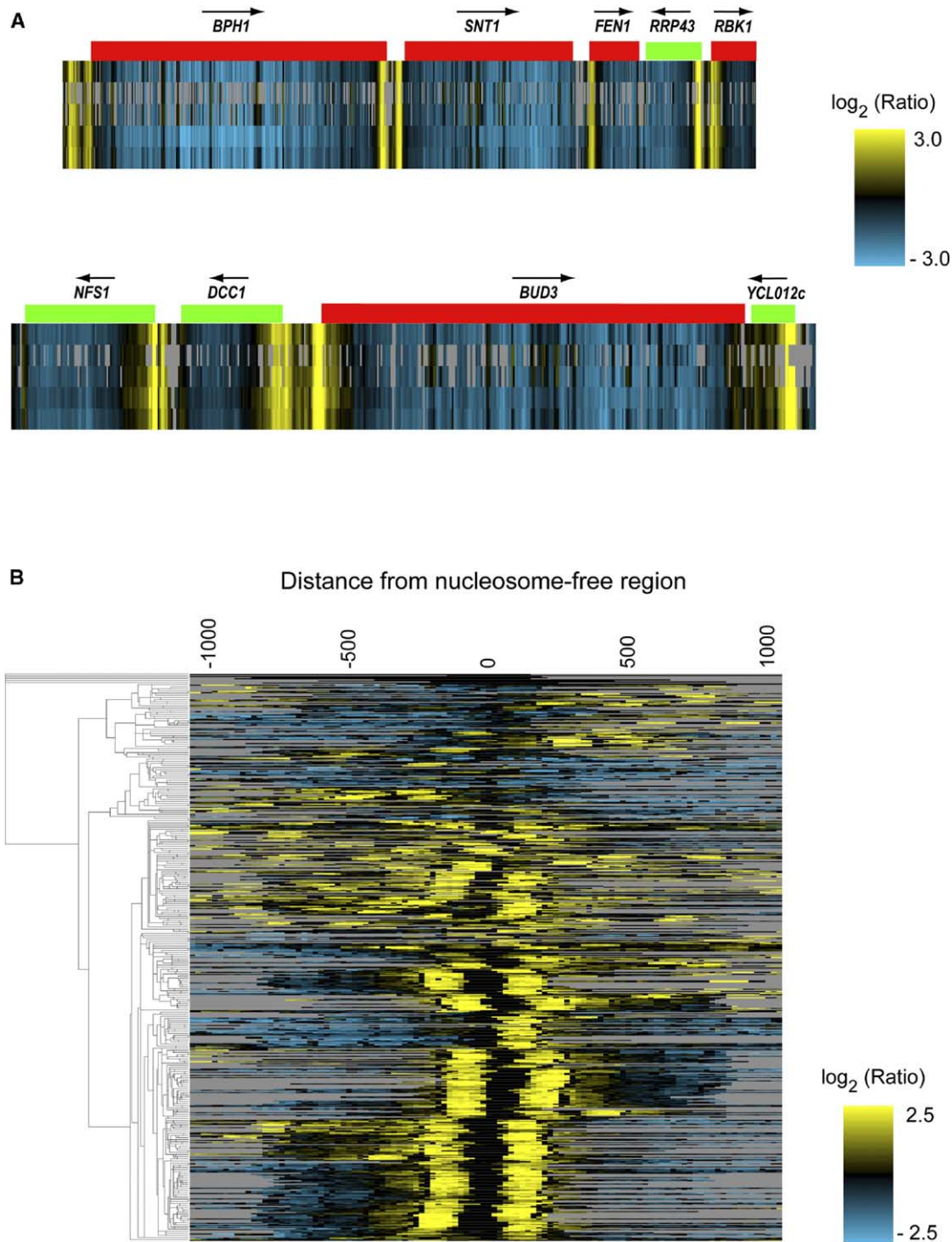


Figure 2. High-Resolution Mapping of H2A.Z Nucleosomes

Shown is a color depiction of ratio of the ChIP signal for mononucleosomal DNA immunoprecipitated using anti-Htz1 antibodies divided by those for DNA extracted from mononucleosomes for regions covered by a high-resolution oligonucleotide tiling microarray.

(A) H2A.Z enrichment in representative euchromatic regions analyzed in Figures 1C and 1D. Shown are the data for five replicate microarray hybridizations. Yellow represents a positive relative enrichment for H2A.Z over the median enrichment versus blue for negative enrichment.

(B) Clustered array dataset centered on nucleosome-free regions (NFRs) of gene promoters. Shown are data from probes from up to 1 kb upstream and 1 kb downstream of the position of the NFR estimated from previous studies (Yuan et al., 2005). Each row represents a single promoter region, and columns correspond to data from microarray oligonucleotides at a given position with respect to the NFR.

III, ORFs annotated as “dubious,” and seven apparently bona fide euchromatic genes (*HIS4*, *POL4*, *ADY2*, *AGP1*, *RPS14A*, *PMP1*, and *YCR006C*). While it is not

obvious why these genes lack H2A.Z in their promoter regions, we note that *YCR006C* contains a tRNA gene in its upstream regions. tRNA genes have been shown

to contain boundary activity (Donze et al., 1999) and have been shown to inhibit expression of adjacent Pol II-transcribed genes (Bolton and Boeke, 2003). Since genes lacking H2A.Z in their promoters represent a small minority, we conclude that H2A.Z generally marks the 5' ends of genes in euchromatin.

Recent work by Yuan and coworkers (2005) demonstrated that nucleosomes are generally uniformly distributed across yeast promoters and ORFs but nearly all yeast genes contain an ~150 bp nucleosome-free region (NFR) centered ~200 bp upstream of the initiation codon. cDNA hybridization studies demonstrated that these regions contain the initiation site for transcription of their associated genes (Yuan et al., 2005). The genes represented in the H2A.Z microarray data were aligned by the center of their NFRs to generate a cluster hierarchy shown in Figure 2B. Remarkably, for about 2/3 of the genes analyzed, the NFR is flanked by two nucleosomes that contain H2A.Z. The remainder of these genes appears either to have H2A.Z present only at one nucleosome or lack H2A.Z entirely for potential reasons explained above (Table S3). Thus, not only does H2A.Z mark the 5' ends of genes, but two positioned H2A.Z nucleosomes typically flank the transcription initiation site. These data demonstrate that H2A.Z nucleosomes are placed in a highly stereotyped and organized manner at the 5' ends of genes.

Active Transcription Is Not Required for H2A.Z Enrichment

The striking localization of H2A.Z at most gene promoters suggested that there could be a relationship between H2A.Z and gene transcription. To address this issue, we selected from the H2A.Z ChIP microarray data those genes that contain two H2A.Z nucleosomes flanking a NFR and compared the levels of H2A.Z enrichment at each of the two nucleosomes to two distinct measurements of transcriptional activity for the corresponding gene (Figure 3). We used genome-scale data from either an analysis of initiation rates (Fraser et al., 2004; Figures 3A and 3C) or RNA polymerase II occupancy (Kim et al., 2004; Figures 3B and 3D). Comparison of H2A.Z enrichment at genes to either data set showed no correlation between H2A.Z enrichment and transcriptional activity. In other words, the transcription rate of a gene does not predict the levels of H2A.Z at a given promoter.

To further assess whether H2A.Z requires active transcription for its selective enrichment at gene promoter regions, we examined several promoter regions under conditions known to produce their tight repression. We first chose to examine the sporulation/meiosis-specific genes *DIT1*, *DIT2*, *HOP1*, and *SPO22* in a haploid strain grown in rich media. These genes are transcriptionally inactive in haploid cells and in nonmeiotic diploid cells (Chu et al., 1998). Additionally, these four occur in two pairs in which their 5' ends flank an intergenic promoter region. Strikingly, we observed peaks of H2A.Z enrichment at both of the shared promoter regions (Figures 4A and 4B). These patterns were not explained by underlying nucleosome density since H3 is relatively evenly distributed across these intervals (Figure S2). To attempt to observe de novo deposition of H2A.Z at

these loci, we constructed a galactose-inducible HA epitope-tagged allele of *HTZ1* with which we could selectively induce or repress the transcription of H2A.Z. As expected, under the repressive glucose condition, virtually no H2A.Z is detectable by ChIP (Figure S3). However, after growth for several generations in galactose, peaks of H2A.Z enrichment were observed at the divergent promoters of both meiotic gene pairs (Figure S3). Thus, H2A.Z can be deposited at inactive genes.

Another region we examined is the highly regulated mating-type specific gene *AGA2*. In yeast, α -specific genes (asgs) such as *AGA2* have been well studied and are known to be active in *MAT α* strains but extremely tightly repressed by the α 2-Mcm1 complex in *MAT α* and *MAT α* / α strains (Galitski et al., 1999). We utilized isogenic strains harboring the chromosomal *HA₃-HTZ1* allele and differing only in the allele present at the mating type locus (*MAT α* or *MAT α*). Using ChIP and QPCR, we observed a peak of H2A.Z signal at *AGA2* in *MAT α* and its continued presence in *MAT α* strains (Figure 4C). Although well above those seen in the ORF of the *BUD3* gene (Figure 4C), H2A.Z levels were approximately 2-fold lower at the repressed *AGA2* locus compared to the active locus even though promoter histone H3 signals were similar in α versus α cells (Figures 4C and S2).

Previous work showed that asg promoters display relative hypoacetylation on the histone H4 tails in *MAT α* strains relative to *MAT α* strains (Deckert and Struhl, 2001). We performed ChIP using antibodies raised against a tetra-acetylated peptide derived from the N-terminal tail of histone H4 (Ac₄H4), and confirmed this result—an approximately 2-fold reduction of acetylation was observed in the *MAT α* strains (Figure 4D). Interestingly, both the positioning and relative level of acetylation in α versus α cells closely parallels those of *HA₃-HTZ1* at *AGA2*, suggesting potential interplay between acetylation and H2A.Z deposition.

Finally, we identified two genes involved in mating in the microarray data that have been shown not to be expressed under vegetative conditions: *FIG2* and *PRM1*. Previous work has shown that expression of these genes only occurs in response to mating pheromone (Erdman et al., 1998; Heiman and Walter, 2000). Analysis of H2A.Z enrichment at these loci revealed peaks in their promoter regions (Figure S4).

Effect of Gene Induction on H2A.Z Levels: Activation of *FIG1* by Mating Pheromone

Our analysis revealed no correlation between H2A.Z levels normalized for nucleosome density and transcription rates or RNA polymerase II occupancies, suggesting no general relationship between transcription and H2A.Z levels. As described in the Introduction, previous studies of H2A.Z levels at *GAL1* and *PHO5* promoters revealed that it decreased upon gene induction, although whether this represented exchange of H2A.Z for H2A or general nucleosome depletion was not determined. In contrast, we observed that while the inactive *AGA2* promoter contains H2A.Z, its levels are higher when the gene is active.

To extend these results, we examined H2A.Z and H3 levels at a gene that is highly inducible by mating pheromone, *FIG1* (Erdman et al., 1998). As shown in Figure

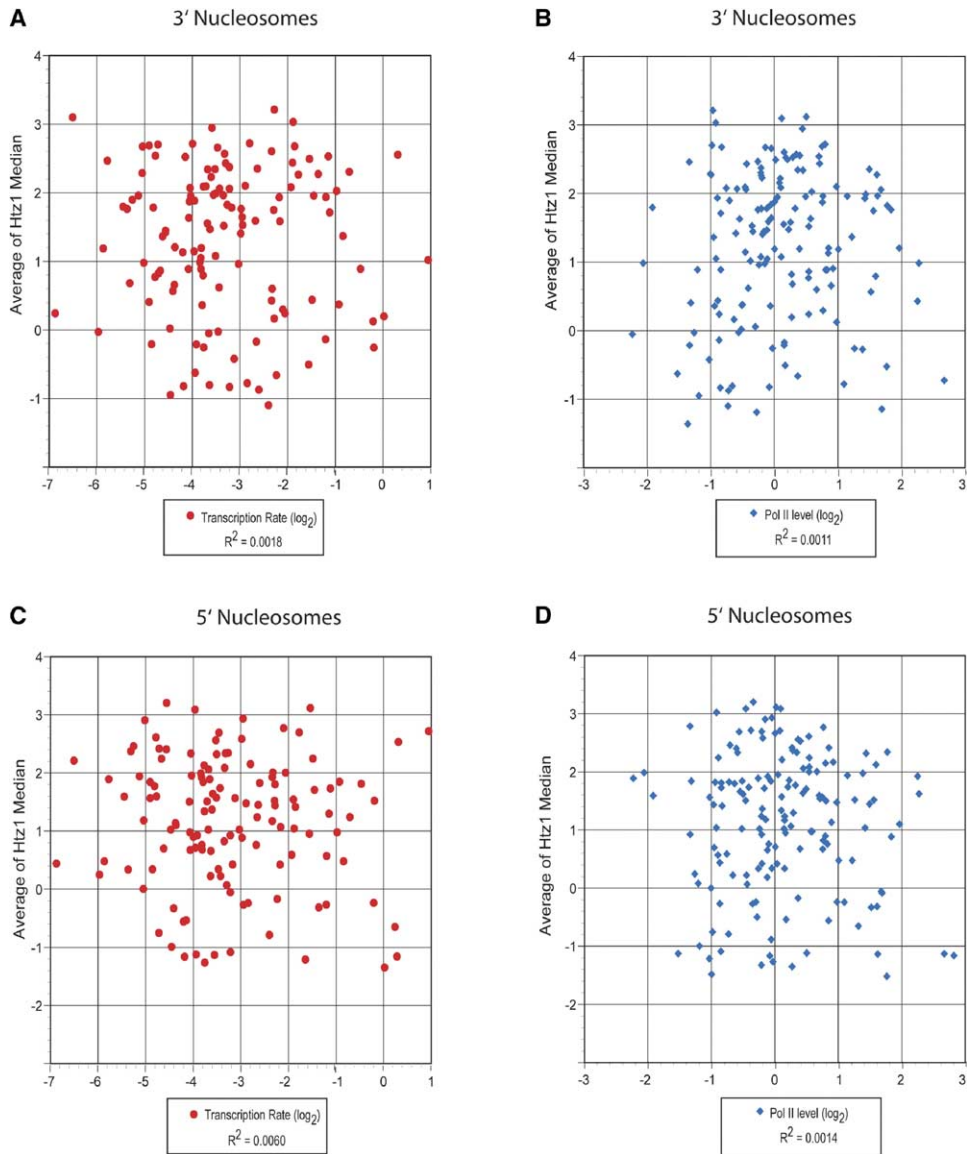


Figure 3. Comparison of H2A.Z Enrichment Normalized for Nucleosome Density with Transcription Rate and RNA Polymerase II Occupancy Shown are plots of promoter H2A.Z enrichments shown in Figure 2 versus calculated transcription rates and RNA polymerase II occupancy as determined by ChIP.

(A) and (B) show plots for H2A.Z nucleosomes 3' of the whereas (C) and (D) show plots for the nucleosomes 5' to the NFR. R² values are shown.

S5, *FIG1* expression is dependent on mating pheromone—treatment of cells with mating pheromone strongly induced mRNA accumulation over a 1 hr time course as determined by quantitative RT-PCR. ChIP analysis revealed that H2A.Z is depleted during gene induction. However, H3 was also depleted from the *FIG1* promoter during the time course such at the 5, 15, and 30 min time points, the ratio of H2A.Z to H3 was constant (Figure S5). At the 60 min time point, an apparent depletion of H2A.Z relative to H3 was observed; however, it seems likely that the promoter H3 signal at this time point was elevated as an artifact of signal from flanking nucleosomes that were not separated by sonication from the promoter nucleosomes prior to ChIP (Figure S5). The H2A.Z signal would not be subject to this problem since H2A.Z nucleosomes are distributed in a

punctate pattern whereas H3-containing nucleosomes are distributed homogeneously. Thus, with the possible exception of this late time point, activation of *FIG1* results in nucleosome loss rather than the specific replacement of H2A.Z with H2A.

Histone Tail Acetylation Is Required for Efficient Recruitment of H2A.Z

We performed a reporter-based genome-wide screen of the *S. cerevisiae* knockout collection to identify genes that antagonize the spread of silencing from the *HMRa* silent mating type cassette (R.M.R. and H.D.M., unpublished data). This screen identified Eaf1, a nonessential component of the essential NuA4 HAT complex and the bromodomain-containing proteins, Bdf1 and Bdf2. Bdf1 is a component of the Swr1 complex re-

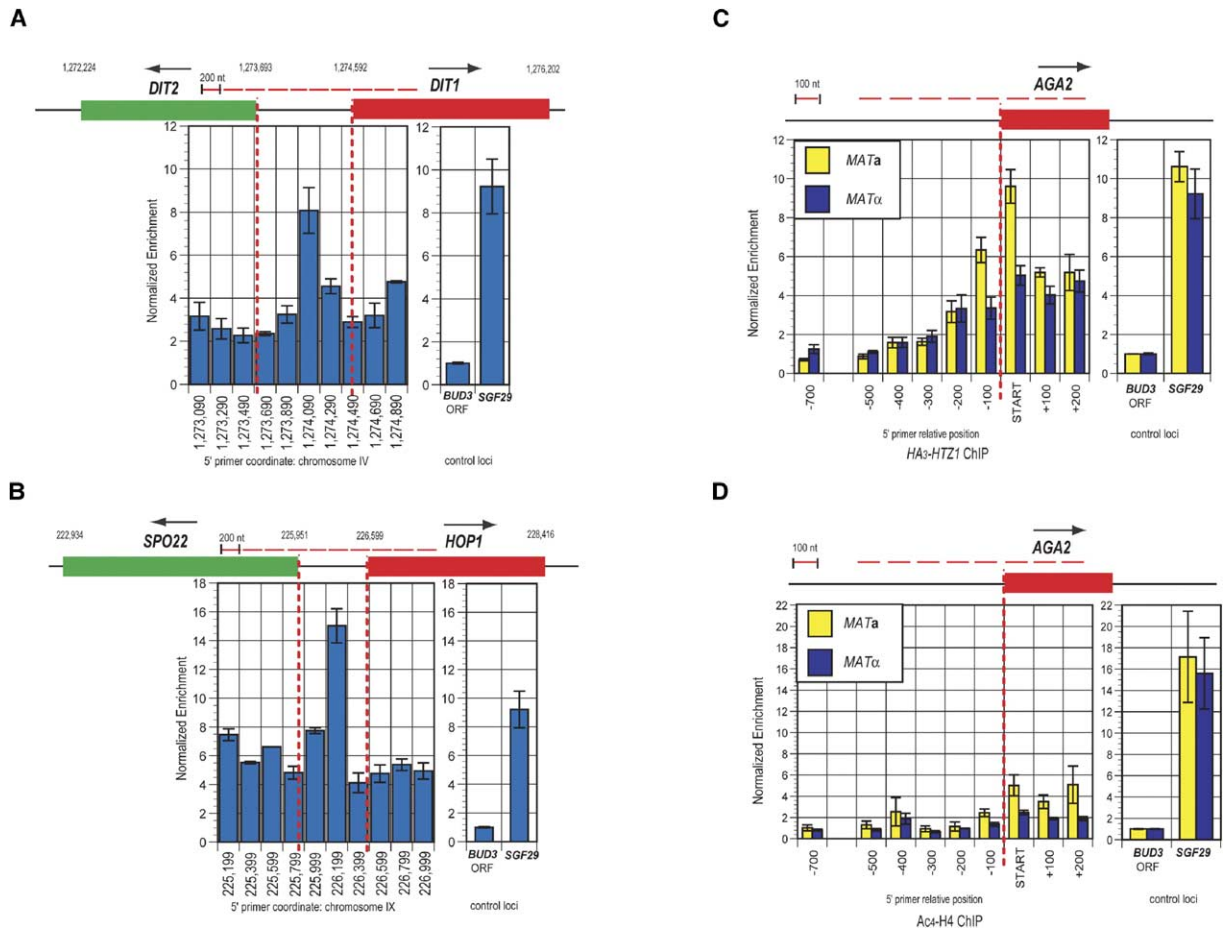


Figure 4. H2A.Z Enrichment at Meiosis-Specific and α -Specific Genes

All enrichment values are triplicate averages of HA_3 -Htz1 or Ac_4 H4 ChIP DNA amounts normalized to the *BUD3* ORF region with SEM error bars. Sidebars show *BUD3* and *SGF29* (positive control) loci.

(A and B) HA_3 -Htz1 enrichment at the *DIT1/DIT2* (A) and *HOP1/SPO22* (B) promoter and ORF regions. QPCR fragments are for consecutive 200 bp segments; dashed lines are drawn through gene initiation codons to their approximate relative position.

(C) HA_3 -Htz1 and (D) Ac_4 H4 normalized enrichment at *AGA2* for *MATα* and *MATα* strains. QPCR probes correspond to consecutive 100 bp segments with the position of the 5' primer relative to the initiation codon of *AGA2* denoted.

responsible for H2A.Z deposition, and both Bdf1 and Bdf2 bind to acetylated histone tails (Ladurner et al., 2003; Matangkasombut and Buratowski, 2003). To test whether histone acetylation is important for H2A.Z deposition, we generated strains bearing the *HA3-HTZ1* allele containing deletions of the genes encoding the H4-specific histone acetyltransferase (HAT) Eaf1 or the H3- and H4-specific HAT Elp3. In addition, we created a strain lacking both HATs. ChIP analysis revealed a dependence upon histone tail acetylation for robust H2A.Z enrichment (Figure 5A). At a majority of loci examined, deletion of *EAF1* resulted in a reproducible defect in H2A.Z levels. The defects varied from approximately 1.5- to 3-fold in magnitude. Likewise, deletion of *ELP3* also led to a defect at most loci, albeit more quantitatively modest than those of the *eaf1Δ* mutant. The severity of the defects in the *eaf1Δ elp3Δ* double mutant is not significantly greater than either of the single deletions (Figure 5A), suggesting Eaf1 and Elp3 may act in the same pathway to mediate H2A.Z deposition.

To further test the role of histone acetylation in H2A.Z deposition, we utilized a series of histone H3 and H4

mutants in which specific target lysine residues have been mutated to arginine which prevents acetylation. We observed a consistent quantitative defect in H2A.Z enrichment values at most of the 10 loci examined (Figures 5B and 5C). In general, the strongest defects were observed in cells harboring the H3-K9R mutant or the H4-K5R,K12R mutant. For the H4-K5R,K12R mutant, we performed ChIP using antibodies against H3 as well and found no differences in nucleosome density at the loci examined in Figure 5C, indicating that the defect in H2A.Z deposition was not caused by general nucleosome loss (Figure S6). Surprisingly, a deletion mutant in the H4 tail displayed a less-severe defect than the H4-K5R,K12R mutant (Figure 5C). The H4-K8R,K16R mutant displayed no defect, indicating that not all mutants in acetylatable tail lysines produce a defect in H2A.Z deposition (Figure 5C).

Bdf1 and Bdf2 Act Redundantly to Promote H2A.Z Deposition

Having established a role for histone tail acetylation for complete H2A.Z deposition, we hypothesized that acet-

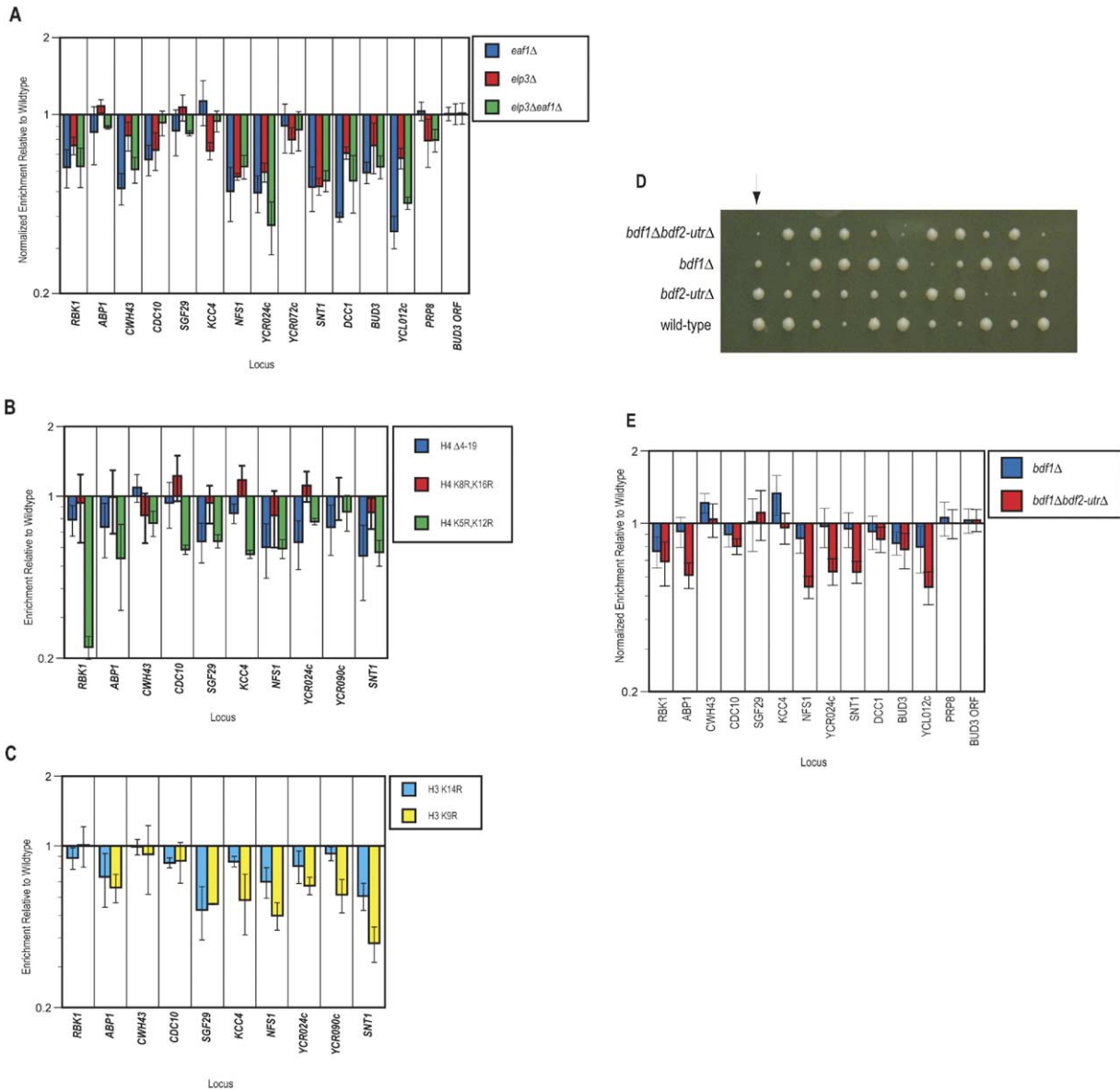


Figure 5. ChIP Analysis of H2A.Z Enrichment at Selected Euchromatic Promoters in Wild-Type, Histone Acetylation-Defective Mutants, and *bdf1Δ* Mutants

(A–C) Triplicate average HA₃-Htz1 enrichment ratios of HAT mutants (A), histone H4 mutants (B), and histone H3 mutants (C) compared to those of wild-type strains plotted on a log scale with SEM error bars.

(D) Tetrad analysis of meiotic products of *BDF1/bdf1Δ BDF2/bdf2-utrΔ* heterozygous diploids. Genotypes of first column of spores are shown. Their phenotypes are representative.

(E) Quadruplicate normalized average H2A.Z enrichment values for mutant compared to wild-type with SEM error bars.

ylation could be acting to recruit targeting of the Swr1 complex via binding of its subunit Bdf1 to acetylated tails. This is an attractive model because in addition to being important for antisilencing, Bdf1 is known to bind preferentially to acetylated forms of histone H4 and is enriched in intergenic regions throughout the genome (Kurdistani et al., 2004). However, ChIP analysis using polyclonal Htz1 antibody raised against the C-terminal tail region showed that a *bdf1Δ* strain has little or no defect in H2A.Z enrichment at euchromatic loci (Figure 5E). We reasoned that this could be due to compensatory

activity by the redundant gene *BDF2*, which when deleted yielded no detectable defect in H2A.Z enrichment (data not shown). Unfortunately, *bdf1Δ bdf2Δ* strains are inviable, precluding a test of this hypothesis using null alleles. Therefore, we elected to generate a “knockdown” allele of *BDF2* by replacing its 3' UTR region with a *MX6* marker cassette. This maneuver has been found to consistently cause destabilization of the cognate mRNA (Schuldiner et al., 2005). We refer to this allele as *bdf2-utrΔ*, and as is the case for the *bdf2Δ*, it also has no defect for H2A.Z enrichment (data not

shown). As seen by tetrad dissection, the *bdf1Δ bdf2-utrΔ* double mutants grow more slowly than either single mutant, indicating a defect produced by *bdf2-utrΔ* (Figure 5D). Examining these strains by ChIP, we found that although *bdf1Δ* cells showed little or no defects in H2A.Z deposition, the *bdf1Δ bdf2-utrΔ* displayed a reproducible defect in H2A.Z deposition at a majority of loci examined (Figure 5E), while no defect was observed in the ORF of the control locus *PRP8*. These experiments clearly demonstrate a dependence on Bdf1 and its redundant homolog Bdf2 for full H2A.Z deposition at the 5' regions of genes. However, since acetylation of promoter nucleosomes generally correlates with transcription (Liu et al., 2005), the requirement for Bdf1/2 and histone tail acetylation for efficient deposition of H2A.Z does not explain how it can be deposited at inactive genes in euchromatin.

Mutagenesis of the *SNT1* Promoter Reveals Sequences Necessary for H2A.Z Deposition In Vivo

One hypothesis for how H2A.Z is deposited at inactive as well as active genes is that there exist specific DNA elements in promoters that program its deposition. Although there is no precedent for a DNA element that specifically induces variant histone deposition, we decided to pursue this model by systematically mutagenizing a typical promoter that contains two positioned H2A.Z nucleosomes (Figure S7). For this analysis, we chose to analyze the *SNT1* promoter region described in Figure 1 because it was well separated from nearby promoters by the relatively large *BPH1* and *SNT1* ORFs.

To localize sequences required for H2A.Z deposition, we divided the *BPH1-SNT1* intergenic region into 75 bp segments and then precisely replaced each segment in the chromosome with a 75 bp fragment of the bacterial cloning vector pBluescript (Figure S7). Mutants in either of two adjacent intervals (termed 5 and 6 in Figure S7) resulted in a modest 2-fold reduction in H2A.Z enrichment (Figure S7). However, a mutant that replaced both intervals resulted in a dramatic defect in H2A.Z enrichment (Figure S7). Interestingly, these two intervals roughly correspond to the nucleosome-free region between the two H2A.Z nucleosomes that lie upstream of the *SNT1* gene. RT-QPCR analysis of *SNT1* expression revealed only a 2-fold drop in *SNT1* mRNA levels (P.D.H. and H.D.M., unpublished data). These data suggested the presence of partially redundant signals for H2A.Z deposition in intervals 5 and 6.

To further define these signals, we constructed 14 additional substitution mutants in the NFR of the *SNT1* promoter (Figure 6A). For these mutants, we replaced varying segments within intervals 5 and 6 with identical-sized segments from the ORF of *BUD3*, which lacks H2A.Z deposition (Figure 1). We examined H2A.Z deposition using primers that span the two flanking positioned H2A.Z nucleosomes. Of the 14 mutants tested, only two, *mu1* and *mu3*, abolished H2A.Z enrichment (Figure 6A). The sequences replaced in *mu3* represent a subset of those in *mu1*, defining the minimal segment that must be mutated to produce a complete loss of H2A.Z deposition in the *SNT1* promoter. Substitution of smaller segments resulted in increased H2A.Z enrichment. For example, *mu4* has the identical 5' endpoint

as *mu3* but substitutes 10 fewer bp on the 3' end and displays robust H2A.Z enrichment (Figure 6A). These 10 bp are therefore critical for H2A.Z deposition in the context of *mu3*. Likewise, *mu10* substitutes 20 bp fewer than *mu3* on the 5' end and shows increased H2A.Z enrichment (Figure 6A), indicating that there are sequences that promote H2A.Z deposition in the 20 bp that distinguish *mu3* from *mu10*. We note that for mutants that display an intermediate level of H2A.Z deposition, our analysis does not distinguish between a decrease in H2A.Z deposition versus a shift in the position of the H2A.Z nucleosomes. Nonetheless, our identification of mutants that eliminate H2A.Z deposition in this region suggest that the segments identified play a role in deposition per se. Taken together, these data suggest the presence of two redundant signals for H2A.Z deposition, one that includes the 10 bp that distinguishes *mu3* from *mu4* and another that includes the 20 bp that distinguishes *mu3* from *mu10*.

A 22 bp Segment from the *SNT1* Promoter Is Sufficient to Induce the Formation of a NFR Flanked by Two H2A.Z Nucleosomes

Our analysis of sequences necessary for H2A.Z deposition at the promoter of *SNT1* identified two discrete regions. We next tested whether these regions also sufficient to promote H2A.Z deposition at a novel site. To date, we have not succeeded in identifying a fragment containing the 20 bp 5' region that is sufficient to promote H2A.Z deposition. Therefore, we focus below on a signal that contains the 3' 10 bp segment hypothesized above to contain a H2A.Z deposition signal.

A magnified view of this 10 bp sequence and flanking sequences is shown in Figure 6B. Two notable features of this sequence are a binding site for the general regulatory factor Reb1 and an adjacent tract of seven dT:dA base pairs. Both sequence elements are disrupted in *mu3* compared to *mu4*. Moreover, previous studies had shown that a similar arrangement of sequences in the yeast *PFY1* promoter was important for the formation of a NFR in that promoter (Angermayr et al., 2003). Therefore, we tested whether a DNA segment containing this region could generate an NFR flanked by H2A.Z nucleosomes when placed elsewhere in the genome.

We inserted the 22 bp segment containing the Reb1 site and (dT:dA)₇ tract at an arbitrarily chosen site in the middle of an inactive gene, *PRM1* (Figure 7A). *PRM1* was selected because it had been shown previously to only be expressed in cells exposed to mating pheromone, and we sought to avoid the potentially complicating effects of transcription on H2A.Z deposition (Heiman and Walter, 2000). Examination of H2A.Z deposition using probes flanking the insertion site revealed robust H2A.Z enrichment in the strain containing the insertion (Figure 7B). Replacement of the three G residues in the Reb1 consensus site abolished the effect of the insertion as did a deletion of the (dT:dA)₇ tract.

To determine whether an NFR was induced by the insertion, we performed nucleosome-scanning analysis (Sekinger et al., 2005) to determine the positions of nucleosomes containing H3 and H2A.Z in the parental strain and the strain containing the insertion. Cross-linked mononucleosomes were immunoprecipitated with

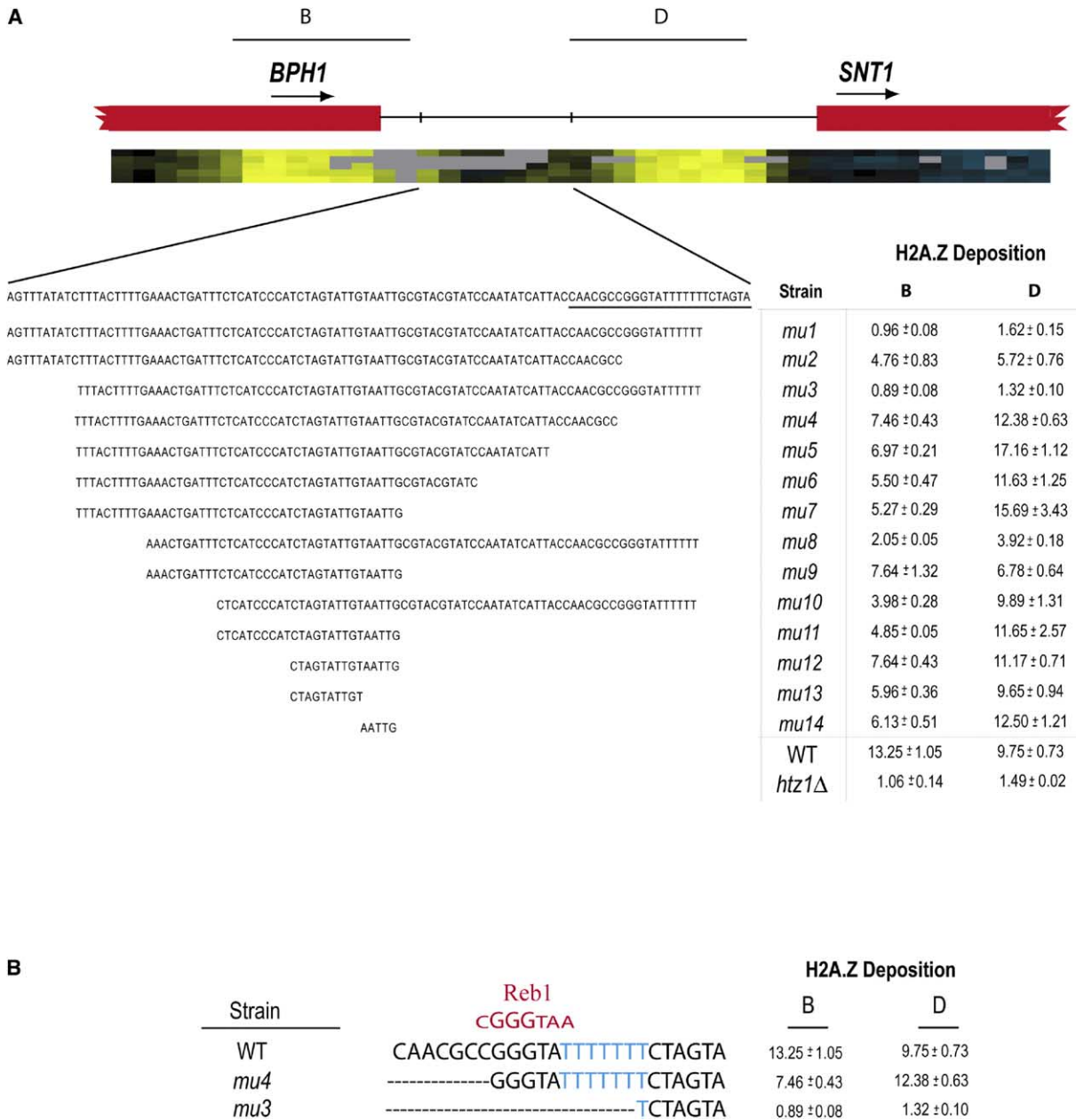


Figure 6. High-Resolution Substitution Mutagenesis of the *BPH1-SNT1* Intergenic Region Defines Sequences Necessary for H2A.Z Deposition In Vivo

(A) Summary of substitution mutants. Shown is the *SNT1-BPH1* interval and microarray data from Figure 2 showing the position of the two H2A.Z nucleosomes that lie in the *SNT1* promoter region. The regions defined as intervals 5 and 6 in Figure S7 were subjected to further mutagenesis. Shown are the sequences that were replaced with heterologous sequences (Table S7). Mutants are designated *mu1-mu14*. To the right are shown the normalized H2A.Z enrichments as determined by standard ChIP and QPCR. Experiments were performed in triplicate. Mean values and their SEM are displayed.

(B) Detail of 3' signal identified by substitution mutagenesis of interval 5. Shown is wild-type sequence corresponding to the right end of interval 5 (underlined in [A]). Consensus DNA binding site for Reb1 is shown; residues shown in large font are invariant (Liaw and Brandl, 1994). Adjacent dT:dA tract is indicated in blue. Shown below are right endpoints of the *mu3* and *mu4* mutants from (A) and their H2A.Z deposition levels. Substituted sequences are indicated by dashes. Mean values and their SEM from (A) are displayed.

antibodies to either H3 or H2A.Z and then analyzed by QPCR analysis using primer pairs that amplified 100 bp segments every 20 bp across the *PRM1* ORF. As shown in Figure 7C, five nucleosomes containing histone H3 were found in the *PRM1* ORF in the parental strain. The arrow in Figure 7C indicates the site of insertion, which

was in the center of the +4 nucleosome. The 22 bp insert had two effects on the nucleosome pattern (Figure 7D). First, it caused a delocalization of the nucleosome pattern in the first part of the *PRM1* ORF. Second, it resulted in a formation of an NFR. This can be deduced by examining the peak-to-peak distance of nucleo-

somes flanking the insertion site, which is 320 bp in the strain containing the insertion versus 180 bp between the center points of the +3 and +4 nucleosomes in the parental strain. Assuming that 147 bp of DNA is wrapped by the yeast histone octamer, one calculates that the insertion caused an expansion of the linker region between these two nucleosomes from approximately 33 bp to 173 bp.

We next determined the positions of H2A.Z nucleosomes in the parental and insertion strains. As shown in Figure 7E, little H2A.Z enrichment was observed in ORF of the *PRM1* gene in the parental strain, as expected. Strikingly, insertion of the 22 bp segment from the *SNT1* gene resulted in the appearance of two positioned variant H2A.Z nucleosomes (Figure 7F). Moreover, the peaks were separated by 320 bp, confirming the formation of an NFR in the insertion strain (Figure 7F). Finally, we examined histone H4 acetylation in the *PRM1* ORF in the strain containing the insertion and found no difference compared to wild-type (P.D.H. and H.D.M., unpublished data), indicating that this DNA signal functions in a distinct pathway from acetylation and Bdf1.

Discussion

Our results show that nucleosomes containing the conserved histone variant H2A.Z occur in euchromatin in a highly organized rather than a random pattern. In particular, the experiments decisively demonstrate that H2A.Z is selectively present at the vast majority of gene promoter regions. Most commonly, it occurs as two positioned nucleosomes that flank a NFR that includes the transcription initiation site. The most striking finding is that H2A.Z enrichment is uncorrelated with transcription rates and is observed at promoters of genes that are not detectably transcribed. The implications of this observation are potentially far reaching, as it indicates that cells can identify the 5' ends of genes in the absence of ongoing transcription. We describe two mechanisms that begin to provide insight into how this remarkable pattern of histone variant deposition occurs. Analysis of the *SNT1* promoter resulted in the identification of a 22 bp bipartite DNA element sufficient to promote H2A.Z deposition when placed in a novel context. This signal contains two necessary elements that are generally conserved in yeast promoters: a binding site for the Myb-related general regulatory factor Reb1 and an (dT:dA)₇ tract. In addition, we demonstrated that H2A.Z deposition is linked to histone acetylation and Bdf1, a double bromodomain protein that binds acetylated histone tails.

H2A.Z Nucleosomes Mark the 5' Ends of Both Active and Inactive Genes in Euchromatin

Our results provide the first single nucleosome-resolution global picture of the deposition pattern of a conserved histone variant. Alignment of the microarray data based on the identified NFR of yeast promoters that includes the transcription initiation site (Yuan et al., 2005) revealed that most euchromatic genes contain two positioned H2A.Z nucleosomes which flank the NFR. Our analysis to date cannot distinguish whether each of these nucleosomes contains two copies of

H2A.Z or one copy of H2A.Z and one copy of H2A. However, it has been suggested based on structural analysis that heteromeric H2A.Z/H2A nucleosomes may be unable to form due to steric clash (Suto et al., 2000). Because one of the two H2A.Z nucleosomes is typically downstream of the initiation site of transcription and one is not, it is unlikely that passage of RNA polymerase alone plays a role in either depositing or removing H2A.Z nucleosomes in general. Indeed, a small group of genes contains only the downstream H2A.Z nucleosome (Figure 2B). It is not yet obvious why these genes differ in their deposition pattern. Consistent with our previous data that indicated the exclusion of H2A.Z nucleosomes from the *HMRa* silent mating-type cassette, the microarray analysis (which was performed in a mating type a strain) reveals an exclusion of H2A.Z from the *HMLα* silent cassette and from subtelomeric regions (see Tables S2 and S3).

Most strikingly, we find that the levels of deposition of H2A.Z in promoters are clearly not correlated with either the transcription rate or RNA polymerase II occupancy of the linked coding sequences (Figure 3). This is in contrast to modifications such as trimethylation of lysine 4 of histone H3 in yeast, which does correlate with transcription rate and typically occurs on the first nucleosomes downstream of the transcription initiation site (Bernstein et al., 2002; Krogan et al., 2003a; Ng et al., 2003b). Indeed, our analysis of genes that are not transcribed and/or tightly repressed demonstrated enrichment of H2A.Z in their promoters. These include two meiotic gene pairs examined in haploid cells in rich media, the a-specific gene *AGA2* assayed in α cells, and two genes only expressed in pheromone-treated cells, *FIG2* and *PRM1*, that were assessed in the absence of pheromone. Although we cannot rule out the possibility that H2A.Z deposition occurs at these genes in response to rare transcription events that produce mRNAs that fail to detectably accumulate, a simpler interpretation of our data is that cells have a transcription-independent mechanism to specify H2A.Z deposition at the 5' ends of genes.

Although H2A.Z can be deposited at inactive genes, our data suggests that transcription can modulate H2A.Z levels in at least two ways. First, at *AGA2*, we observed higher H2A.Z levels when the gene was active than when it was inactive. Second, at *FIG1*, we observed that activation resulted in concomitant depletion of H2A.Z and H3, consistent with the removal of variant octamers. Since the relative levels of H2A.Z and transcription are uncorrelated when considering large numbers of genes (Figure 3), it seems likely that transcription modulates the relative amounts of H2A.Z variant nucleosomes differently at different genes. Further work will be needed to define the relationships between transcription and H2A.Z promoter marking. Nonetheless, our results demonstrate that for cells to identify the 5' ends of genes and deposit H2A.Z, genes need not be transcribed.

Histone Tail Acetylation and Bdf1 Promote Deposition of H2A.Z

Our genetic experiments led us to investigate the potential connection between histone tail acetylation and H2A.Z deposition. ChIP analyses demonstrated that for

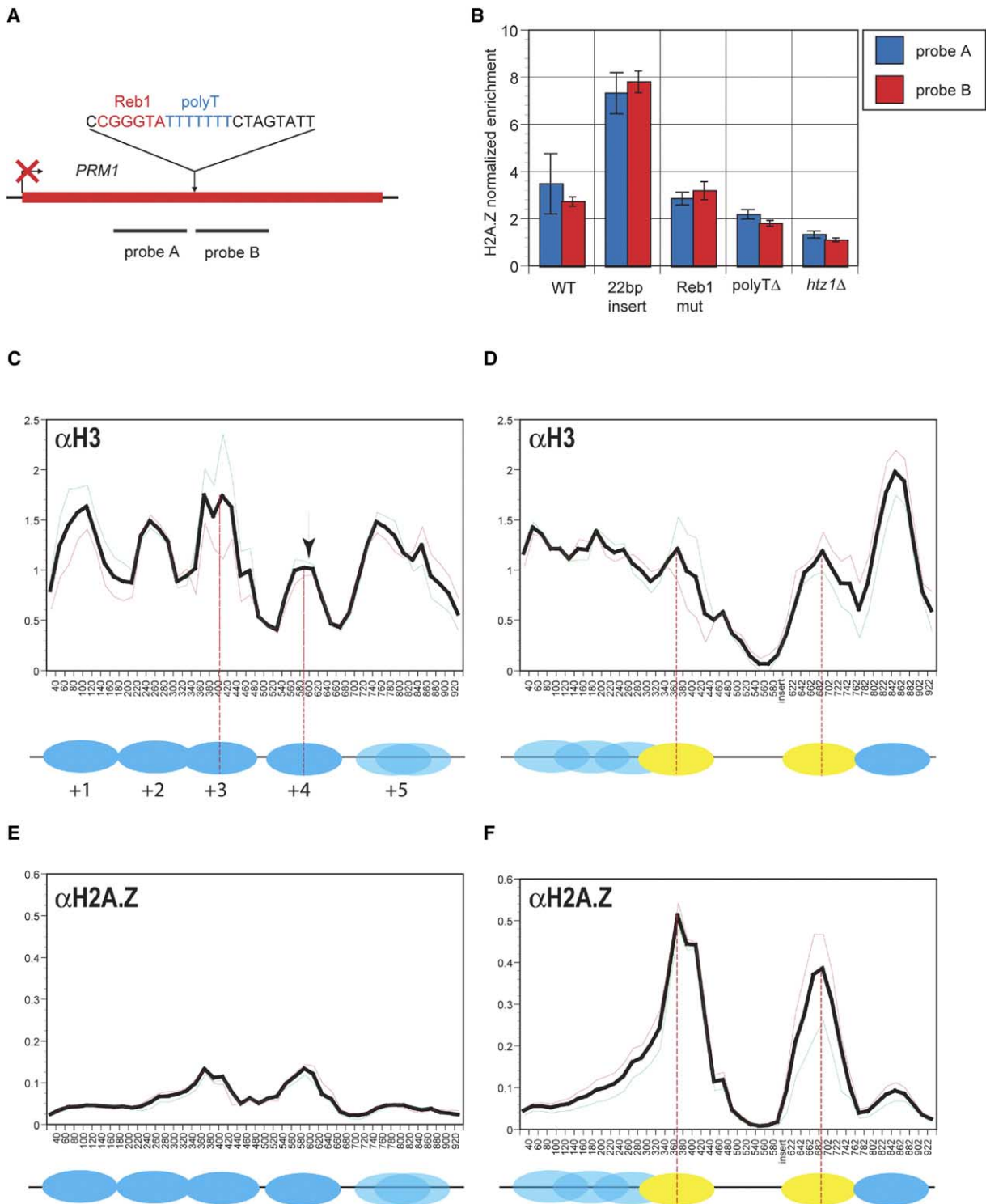


Figure 7. A 22 bp Bipartite DNA Sequence from the *SNT1* Promoter Sufficient to Direct the Deposition of Two H2A.Z Nucleosomes and the Formation of a Nucleosome-Free Region

(A) Experimental Design. Shown is the sequence from the *SNT1* promoter and its arbitrarily chosen site of insertion in the *PRM1* ORF. PCR probes used in (B) are indicated.

(B) Demonstration that 22 bp element from *SNT1* promoter is sufficient to promote H2A.Z deposition: standard ChIP analysis. Shown are the normalized H2A.Z enrichment values for the indicated probes for a wild-type strain and three isogenic strains containing either the 22 bp insertion shown in (A), a GGG→TAA mutant in the Reb1 site, or a mutant that precisely deletes the T tract. Experiments were performed in triplicate. Mean values and their SEM are displayed.

(C) Nucleosome-scanning analysis of histone H3 positions in the *PRM1* ORF in wild-type cells. Shown is the analysis of mononucleosomes

various defects in histone tail acetylation, whether produced by mutation of acetylated lysines or deletion of genes encoding histone acetyltransferases, there is a moderate decrease in H2A.Z at most sites assayed. The quantitative rather than qualitative defect in H2A.Z deposition in these mutant backgrounds may reflect either a partial dependence on histone tail acetylation for deposition or that histone acetylation was only partially eliminated in our experiments. Distinguishing between these two possibilities is not trivial since the H3 and H4 N-terminal tails are together essential for viability (Ling et al., 1996). Moreover, cells lacking the catalytic subunit of the NuA4 HAT and cells lacking both the Gcn5 and Sas3 HATs are inviable (Clarke et al., 1999; Howe et al., 2001). We also note that the *in vivo* deposition assays used here do not measure the rate of H2A.Z deposition. Therefore, the modest defects observed in acetylation mutants at steady state may reflect a more profound defect in the rate of deposition, especially if one considers that as few as one exchange event at a nucleosome per cell cycle might be sufficient to produce wild-type levels of H2A.Z.

We find that the bromodomain proteins Bdf1 and Bdf2 act redundantly to promote H2A.Z deposition. Bdf1 is a subunit of both the Swr1 complex that deposits H2A.Z *in vivo* and is also associated with TFIID. Because Bdf1 contains two bromodomains and selectively binds acetylated versions of histone H4, we suggest that Bdf1 recognition of acetylated histone tails promotes recruitment of the Swr1 complex and deposition of H2A.Z. *In vitro* studies of the purified Swr1 complex and acetylated nucleosomal substrates will be required to confirm this model. It is notable that the H4-K8R, K16R mutation did not affect H2A.Z deposition: recent work has shown that deacetylation of H4-K16 is actually necessary for the association of Bdf1 with chromatin *in vivo* (Kurdistani et al., 2004). Consistent with these observations, recent studies of histone acetylation patterns at the mononucleosome level demonstrated that the two nucleosomes flanking the NFR have a unique acetylation pattern (Liu et al., 2005). In particular, these nucleosomes are both highly deacetylated on H4-K8 and 16, and this deacetylation domain occurs independently of transcription level, thereby precisely paralleling the H2A.Z localization pattern presented here. Moreover, the nucleosome downstream of the NFR is acetylated on H3-K9,14 and H4-K5,12. It is unlikely to be coincidental that lysine-to-arginine mutation of the residues that are deacetylated on the NFR-

Table 1. Comparison of Histone Tail Acetylation Patterns at NFR-Flanking Nucleosomes and Residues Required for H2A.Z Deposition

Modification	Present at NFR-Flanking Nucleosomes?	Required for H2A.Z Deposition?
Ac-H3-K9	Yes	Yes
Ac-H3-K14	Yes	Yes
Ac-H4-K5	Yes	Yes ^a
Ac-H4-K8	No	No
Ac-H4-K12	Yes	Yes ^a
Ac-H4-K16	No	No

^aBased on H4-K5,12 double mutant.

flanking nucleosomes does not affect H2A.Z deposition, while mutation of acetylated residues inhibits H2A.Z deposition (Table 1). Together with the data showing that Bdf1 binding to chromatin is inhibited by H4-K16 acetylation, these results are consistent with a direct role for Bdf1 in recognizing the acetylation patterns of the NFR-flanking nucleosomes to promote H2A.Z deposition. However, since acetylation of the nucleosome downstream of the NFR correlates with transcription rates (Liu et al., 2005), efficient deposition of H2A.Z at highly deacetylated inactive promoters must involve mechanisms that would not in principle depend on ongoing transcription.

Identification of a Bipartite DNA Signal Sufficient to Induce H2A.Z Deposition

We have defined one such mechanism, namely the existence of DNA signals that program H2A.Z deposition. Our analysis of the *SNT1* promoter revealed two segments of DNA that appear to function redundantly since mutations in two segments with the NFR were necessary to eliminate H2A.Z deposition. We showed that the 3' signal, which contains a site for the Myb-related general regulatory factor Reb1 and an adjacent (dT:dA)₇ tract, was sufficient to induce the formation of an NFR and the replacement of H2A with H2A.Z in the two flanking nucleosomes when placed into the middle of the coding sequence of inactive *PRM1* gene. Both the Reb1 site and (dT:dA)₇ motif were found to be necessary for H2A.Z deposition.

Reb1 was originally identified as an abundant nuclear protein involved in rDNA transcriptional termination but was subsequently shown to associate with a large

immunoprecipitated using anti-H3 antibodies. The y axis corresponds to a mononucleosome:genomic ratio normalized to the median. Plotted is a four-window moving average for two replicate experiments (thin red and green lines) and their averages (thick black line). The moving average is plotted such that the first data point is relative to position 30, which is the center of the window. Indicated below are deduced positions of nucleosomes. Also marked is the site of the 22 bp insertion from the *SNT1* promoter, which was placed into the middle of the +4 nucleosome. Peak-to-peak distance between the two nucleosomes flanking the site of insertion is indicated.

(D) Nucleosome-scanning analysis of histone H3 positions in the *PRM1* ORF in cells containing the 22 bp insertion. Strain containing the insertion was analyzed as in (C). Peak-to-peak distance between the two nucleosomes flanking the site of insertion is indicated.

(E) Nucleosome-scanning analysis of histone H2A.Z positions in the *PRM1* ORF in wild-type cells. Mononucleosomal material from the indicated strains was immunoprecipitated with anti-H2A.Z antibodies and analyzed as in (C). The y axis corresponds to a mononucleosome:genomic ratio.

(F) Nucleosome-scanning analysis of histone H2A.Z positions in the *PRM1* ORF in cells containing the 22 bp insertion. Mononucleosomal material from the indicated strains was immunoprecipitated with anti-H2A.Z antibodies and analyzed as in (E). The y axis is the same as in (C). Peak-to-peak distance between the two nucleosomes flanking the site of insertion is indicated.

number of yeast promoter regions (Ju et al., 1990). Recent studies of the conservation of the Reb1 DNA binding motif have shown that it is the single most conserved motif found in yeast promoters and is even more conserved across species than the TATA box (Elemento and Tavazoie, 2005). Several studies have shown that tethering of Reb1 or related Myb-family general regulatory factors (Rap1, Abf1, or Tbf1) to DNA can prevent the spread of silent chromatin, but the mechanism remains unknown (Fourel et al., 2002; Yu et al., 2003). Given our results, it could be that this property of these factors involves the induction of a NFR and/or the deposition of H2A.Z nucleosomes. Consistent with this possibility, there is a near match to the Abf1 binding consensus in the region of the *SNT1* NFR that contains the 5' signal for H2A.Z deposition (P.D.H. and H.D.M., unpublished data).

The second motif that we found to be important for H2A.Z deposition is a tract of dT:dA base pairs which have been noted to be common in yeast promoters, particularly in NFRs (Yuan et al., 2005). Studies of global nucleosome density have also shown that the abundance of motifs containing dT:dA tracts correlate with nucleosome depletion from promoters (Bernstein et al., 2004; Lee et al., 2004). These studies concluded that promoters show transcription-independent reductions in nucleosome density compared coding sequences, but this conclusion has been questioned on technical grounds (Pokholok et al., 2005). Our study is relevant to this issue as it shows the functional importance of an element containing a dT:dA tract flanked by a site for Reb1 in the formation of NFR. Our data may also be relevant to the recent proposal that dT:dA tracts promote the formation of NFRs in vivo because of their intrinsic nucleosome excluding properties in vitro (Sekinger et al., 2005). Although further work is necessary to understand how it functions, it seems unlikely that a sequence as short as 22 bp could act to program the formation of an ~170 bp NFR purely because of its intrinsic properties.

Although both Reb1 sites and dT:dA tracts are common features of yeast promoters, we do not yet know whether this is the sole type of DNA element that programs H2A.Z deposition at promoters. As mentioned above, other Myb-related factors might also be expected to play a role. A previous study identified a Reb1 site and an adjacent dT:dA tract in the NFR in the promoter of the yeast *PFY1* gene (Angermayr et al., 2003). This work showed that mutation of the Reb1 site eliminated the NFR; the role of the adjacent dT:dA tract was not assessed. Thus, it may be that Reb1 is generally important for the formation of NFRs in promoters. This raises the question of whether Reb1 promotes H2A.Z deposition and NFR formation through independent or coupled mechanisms. Our preliminary studies show that deletion of *HTZ1* or *SWR1* does not prevent the formation of the NFR in the strain containing the 22 bp insertion into *PRM1* (P.D.H. and H.D.M., unpublished data). Thus, the 22 bp element either promotes NFR formation and H2A.Z independently (e.g., via recruitment of different factors) or the formation of the NFR itself induces H2A.Z deposition. Regardless of the specific mechanisms involved, our studies indicate that DNA- and histone-based mechanisms allow cells to

mark the 5' ends of genes and preserve their euchromatic state.

Experimental Procedures

Yeast Strains

Strains used in these studies are described in Table S5.

Mapping DNA Sequences Necessary for H2A.Z Deposition

Chromosomal mutations were created as described (Storici et al., 2003). Heterologous sequences used are described in Table S7. Different sequences were used in Figure S7 and Figure 6 to ensure that the results were not dependent on the particular sequence used to replace *SNT1* sequences.

Galactose Induction of HA-Htz1 Expression

Cultures were grown at 30°C. Strains bearing an HA₃ epitope-tagged allele of *HTZ1* driven by the *GAL1* promoter at the endogenous *HTZ1* locus were grown to saturation in YPAD, then diluted to an A_{600} of 0.1, and outgrown in YEP containing 2% glucose to an A_{600} of 0.6. Fifty milliliters of the cultures were crosslinked and harvested. The remaining cells were washed twice in water and added to YEP containing 2% galactose and 2% raffinose to an approximate A_{600} of 0.001 and grown for 2 days. These cultures were then back diluted to fresh YEP containing 2% galactose and 2% raffinose to an A_{600} OD of 0.1 and grown to an A_{600} of 0.6, crosslinked, and harvested. Three absorbance units were harvested from each and analyzed by immunoblotting with antibodies against H2A.Z.

Induction of *FIG1* by Mating Pheromone

A wild-type *MATa* strain was grown in YPAD at 30°C overnight, diluted to an A_{600} of 0.1, and grown to an A_{600} of 0.6. Thirty OD units were crosslinked and harvested for ChIP, and three OD units were harvested for total RNA isolation and RT-QPCR analysis of transcript levels using gene-specific primers for *FIG1* and *ACT1*. The remaining culture was split four ways and α factor was added to a concentration of 10 μ M to each and grown to the appropriate time point (5 min, 15 min, 30 min, or 1 hr), whereupon 30 and 3 OD of cells respectively were harvested as described above for ChIP and RT-QPCR analysis.

Mononucleosome Preparation for Microarray and Nucleosome Scanning Experiments

Mononucleosomes were prepared as described (Liu et al., 2005).

Chromatin Immunoprecipitation

ChIP procedures were as in Meneghini et al. (2003) except for microarray and nucleosome scanning experiments, which were performed as described by Liu et al. (2005) and Sekinger et al. (2005), respectively.

High-Density Microarray Tiling Analysis of H2A.Z Deposition Profile

The yeast strain used was BY4741. Hybridization and analysis was performed as described (Liu et al., 2005).

Supplemental Data

Supplemental Data include seven figures and seven tables and can be found with this article online at <http://www.cell.com/cgi/content/full/123/2/233/DC1/>.

Acknowledgments

We are grateful to S. Dent for histone point mutants. This work was supported by grants from the NIH-NIGMS (H.D.M., S.L.S., O.J.R.), the Packard Foundation (H.D.M.), the Bauer Center (S.L.S., O.J.R.), and the Burroughs-Wellcome Fund (M.D.M.). We thank W. Marshall for critical reading of the manuscript, R. Wu for pointing out the Reb1 site, and S. Johnson and J. DeRisi for support and advice. Author contributions are as follows: R.M.R. performed the experiments shown in Figures 1C, 1D, 4, 5, S1, S2, S3, S5, and S6. P.D.H. performed the experiments shown in Figures 6, 7, and S7. M.Z.B. and M.D.M. performed the experiments shown in Figures 1A and

1B. C.L.L. and O.J.R. performed the experiments shown in [Figures 2, 3, and S4](#). R.M.R., P.D.H., O.J.R., and H.D.M. wrote the paper.

Received: May 15, 2005
Revised: October 3, 2005
Accepted: October 5, 2005
Published: October 20, 2005

References

- Angermayr, M., Oechsner, U., and Bandlow, W. (2003). Reb1p-dependent DNA bending effects nucleosome positioning and constitutive transcription at the yeast profilin promoter. *J. Biol. Chem.* **278**, 17918–17926.
- Bernstein, B.E., Humphrey, E.L., Erlich, R.L., Schneider, R., Bouman, P., Liu, J.S., Kouzarides, T., and Schreiber, S.L. (2002). Methylation of histone H3 Lys 4 in coding regions of active genes. *Proc. Natl. Acad. Sci. USA* **99**, 8695–8700.
- Bernstein, B.E., Liu, C.L., Humphrey, E.L., Perlestein, E.O., and Schreiber, S.L. (2004). Global nucleosome occupancy in yeast. *Genome Biol.* **5**, R62.
- Bolton, E.C., and Boeke, J.D. (2003). Transcriptional interactions between yeast tRNA genes, flanking genes and Ty elements: a genomic point of view. *Genome Res.* **13**, 254–263.
- Chu, S., DeRisi, J., Eisen, M., Mulholland, J., Botstein, D., Brown, P.O., and Herskowitz, I. (1998). The transcriptional program of sporulation in budding yeast. *Science* **282**, 699–705.
- Clarke, A.S., Lowell, J.E., Jacobson, S.J., and Pillus, L. (1999). Esa1p is an essential histone acetyltransferase required for cell cycle progression. *Mol. Cell. Biol.* **19**, 2515–2526.
- Deckert, J., and Struhl, K. (2001). Histone acetylation at promoters is differentially affected by specific activators and repressors. *Mol. Cell. Biol.* **21**, 2726–2735.
- Donze, D., Adams, C.R., Rine, J., and Kamakaka, R.T. (1999). The boundaries of the silenced HMR domain in *Saccharomyces cerevisiae*. *Genes Dev.* **13**, 698–708.
- Elemento, O., and Tavazoie, S. (2005). Fast and systematic genome-wide discovery of conserved regulatory elements using a non-alignment based approach. *Genome Biol.* **6**, R18.
- Erdman, S., Lin, L., Malczynski, M., and Snyder, M. (1998). Pheromone-regulated genes required for yeast mating differentiation. *J. Cell Biol.* **140**, 461–483.
- Fourel, G., Miyake, T., Defossez, P.A., Li, R., and Gilson, E. (2002). General regulatory factors (GRFs) as genome partitioners. *J. Biol. Chem.* **277**, 41736–41743.
- Fraser, H.B., Hirsh, A.E., Giaever, G., Kumm, J., and Eisen, M.B. (2004). Noise minimization in eukaryotic gene expression. *PLoS Biol.* **2**, e137. 10.1371/journal.pbio.0020137.
- Galitski, T., Saldanha, A.J., Styles, C.A., Lander, E.S., and Fink, G.R. (1999). Ploidy regulation of gene expression. *Science* **285**, 251–254.
- Heiman, M.G., and Walter, P. (2000). Prm1p, a pheromone-regulated multispinning membrane protein, facilitates plasma membrane fusion during yeast mating. *J. Cell Biol.* **151**, 719–730.
- Howe, L., Auston, D., Grant, P., John, S., Cook, R.G., Workman, J.L., and Pillus, L. (2001). Histone H3 specific acetyltransferases are essential for cell cycle progression. *Genes Dev.* **15**, 3144–3154.
- Hwang, W.W., Venkatasubrahmanyam, S., Ianculescu, A.G., Tong, A., Boone, C., and Madhani, H.D. (2003). A conserved RING finger protein required for histone H2B monoubiquitination and cell size control. *Mol. Cell* **11**, 261–266.
- Ju, Q.D., Morrow, B.E., and Warner, J.R. (1990). REB1, a yeast DNA-binding protein with many targets, is essential for growth and bears some resemblance to the oncogene myb. *Mol. Cell. Biol.* **10**, 5226–5234.
- Kim, M., Krogan, N.J., Vasiljeva, L., Rando, O.J., Nedeá, E., Greenblatt, J.F., and Buratowski, S. (2004). The yeast Rat1 exonuclease promotes transcription termination by RNA polymerase II. *Nature* **432**, 517–522.
- Kimura, A., Umehara, T., and Horikoshi, M. (2002). Chromosomal gradient of histone acetylation established by Sas2p and Sir2p functions as a shield against gene silencing. *Nat. Genet.* **32**, 370–377.
- Kobor, M.S., Venkatasubrahmanyam, S., Meneghini, M.D., Gin, J.W., Jennings, J., Link, A.J., Madhani, H.D., and Rine, J. (2004). A protein complex containing the conserved Swi2/Snf2-related ATPase Swr1p deposits histone variant H2A.Z into euchromatin. *PLoS Biol.* **2**, e131. 10.1371/journal.pbio.0020131.
- Krogan, N.J., Dover, J., Wood, A., Schneider, J., Heidt, J., Boateng, M.A., Dean, K., Ryan, O.W., Golshani, A., Johnston, M., et al. (2003a). The Paf1 complex is required for histone H3 methylation by COMPASS and Dot1p: Linking transcriptional elongation to histone methylation. *Mol. Cell* **11**, 721–729.
- Krogan, N.J., Keogh, M.C., Datta, N., Sawa, C., Ryan, O.W., Ding, H., Haw, R.A., Pootoolal, J., Tong, A., Canadien, V., et al. (2003b). A Snf2 family ATPase complex required for recruitment of the histone H2A variant Htz1. *Mol. Cell* **12**, 1565–1576.
- Kurdistani, S.K., Tavazoie, S., and Grunstein, M. (2004). Mapping global histone acetylation patterns to gene expression. *Cell* **117**, 721–733.
- Ladurner, A.G., Inouye, C., Jain, R., and Tjian, R. (2003). Bromodomains mediate an acetyl-histone encoded antisilencing function at heterochromatin boundaries. *Mol. Cell* **11**, 365–376.
- Lee, C.K., Shibata, Y., Rao, B., Strahl, B.D., and Lieb, J.D. (2004). Evidence for nucleosome depletion at active regulatory regions genome-wide. *Nat. Genet.* **36**, 900–905.
- Liaw, P.C., and Brandl, C.J. (1994). Defining the sequence specificity of the *Saccharomyces cerevisiae* DNA binding protein REB1p by selecting binding sites from random-sequence oligonucleotides. *Yeast* **10**, 771–787.
- Ling, X., Harkness, T.A., Schultz, M.C., Fisher-Adams, G., and Grunstein, M. (1996). Yeast histone H3 and H4 amino termini are important for nucleosome assembly in vivo and in vitro: redundant and position-independent functions in assembly but not in gene regulation. *Genes Dev.* **10**, 686–699.
- Liu, C.L., Kaplan, T., Kim, M., Buratowski, S., Schreiber, S.L., Friedman, N., and Rando, O.J. (2005). Single-nucleosome mapping of histone modifications in *S. cerevisiae*. *PLoS Biol.* **3**, e328. 10.1371/journal.pbio.0030328.
- Matangkasombut, O., and Buratowski, S. (2003). Different sensitivities of bromodomain factors 1 and 2 to histone H4 acetylation. *Mol. Cell* **11**, 353–363.
- Meneghini, M.D., Wu, M., and Madhani, H.D. (2003). Conserved histone variant H2A.Z protects euchromatin from the ectopic spread of silent heterochromatin. *Cell* **112**, 725–736.
- Mizuguchi, G., Shen, X., Landry, J., Wu, W.H., Sen, S., and Wu, C. (2004). ATP-driven exchange of histone H2AZ variant catalyzed by SWR1 chromatin remodeling complex. *Science* **303**, 343–348.
- Ng, H.H., Ciccone, D.N., Morshead, K.B., Oettinger, M.A., and Struhl, K. (2003a). Lysine-79 of histone H3 is hypomethylated at silenced loci in yeast and mammalian cells: a potential mechanism for position-effect variegation. *Proc. Natl. Acad. Sci. USA* **100**, 1820–1825.
- Ng, H.H., Robert, F., Young, R.A., and Struhl, K. (2003b). Targeted recruitment of Set1 histone methylase by elongating Pol II provides a localized mark and memory of recent transcriptional activity. *Mol. Cell* **11**, 709–719.
- Pokholok, D.K., Harbison, C.T., Levine, S., Cole, M., Hannett, N.M., Lee, T.I., Bell, G.W., Walker, K., Rolfe, P.A., Herbolsheimer, E., et al. (2005). Genome-wide map of nucleosome acetylation and methylation in yeast. *Cell* **122**, 517–527.
- Santisteban, M.S., Kalashnikova, T., and Smith, M.M. (2000). Histone H2A.Z regulates transcription and is partially redundant with nucleosome remodeling complexes. *Cell* **103**, 411–422.
- Santos-Rosa, H., Bannister, A.J., Dehe, P.M., Geli, V., and Kouzarides, T. (2004). Methylation of H3 lysine 4 at euchromatin promotes Sir3p association with heterochromatin. *J. Biol. Chem.* **279**, 47506–47512.
- Schuldiner, M., Collins, S.R., Thompson, N.J., Denic, V., Bhamidi-

pati, A., Punna, T., Ihmels, J., Andrews, B., Boone, C., Greenblatt, J.F., et al. (2005). Exploration of the function and organization of the yeast early secretory pathway through an epistatic miniarray profile. *Cell*, in press.

Sekinger, E.A., Moqtaderi, Z., and Struhl, K. (2005). Intrinsic histone-DNA interactions and low nucleosome density are important for preferential accessibility of promoter regions in yeast. *Mol. Cell* 18, 735–748.

Storici, F., Durham, C.L., Gordenin, D.A., and Resnick, M.A. (2003). Chromosomal site-specific double-strand breaks are efficiently targeted for repair by oligonucleotides in yeast. *Proc. Natl. Acad. Sci. USA* 100, 14994–14999.

Suka, N., Luo, K., and Grunstein, M. (2002). Sir2p and Sas2p oppositely regulate acetylation of yeast histone H4 lysine16 and spreading of heterochromatin. *Nat. Genet.* 32, 378–383.

Suto, R.K., Clarkson, M.J., Tremethick, D.J., and Luger, K. (2000). Crystal structure of a nucleosome core particle containing the variant histone H2AZ. *Nat. Struct. Biol.* 7, 1121–1124.

van Leeuwen, F., Gafken, P.R., and Gottschling, D.E. (2002). Dot1p modulates silencing in yeast by methylation of the nucleosome core. *Cell* 109, 745–756.

Yu, Q., Qiu, R., Foland, T.B., Griesen, D., Galloway, C.S., Chiu, Y.H., Sandmeier, J., Broach, J.R., and Bi, X. (2003). Rap1p and other transcriptional regulators can function in defining distinct domains of gene expression. *Nucleic Acids Res.* 31, 1224–1233.

Yuan, G.C., Liu, Y.J., Dion, M.F., Slack, M.D., Wu, L.F., Altschuler, S.J., and Rando, O.J. (2005). Genome-scale identification of nucleosome positions in *S. cerevisiae*. *Science* 309, 626–630.

Accession Numbers

Microarray data has been deposited in the NIH GEO database (accession number GSE3411).